ACS Catalysis

Research Article

pubs.acs.org/acscatalysis

Toward More Complete Descriptors of Reactivity in Catalysis by Solid Acids

Prashant Deshlahra[†] and Enrique Iglesia*[,†,‡]

[†]Department of Chemical and Biomolecular Engineering, University of California at Berkeley, Berkeley, California 94720, United States

[‡]Chemical Sciences Division, E.O. Lawrence Berkeley National Laboratory, Berkeley, California 94720, United States

Supporting Information

ABSTRACT: Density functional theory and classical electrostatics are used to develop reactivity descriptors for catalysis by solid acids. Acid strength, as deprotonation energies (DPE), reflects the charge reorganization required to disrupt covalent OH bonds in inorganic acids and the electrostatic forces that resist the separation of protons from conjugate anions. Both charge reorganization (covalent) and electrostatic (ionic) components vary monotonically with DPE on solid acids with different heteroatoms within a given type of oxide framework, but their relative contributions differ among different acid types. Ion-pair transition states recover predominantly the ionic part of the DPE, and the extent to which they recover each component is a unique property of a transition state and thus of an acid-catalyzed reaction, independent of the acid strength or type. These fractional recoveries, together with the ionic and covalent DPE components, a unique property of a solid acid, provide a general and complete descriptor of reactivity, which we illustrate here for diverse reactions (proton shuttling, H_2O elimination, methyl shift, ring contraction) on several types of solid acids (Mo- and W-based polyoxometalate clusters with S, P, Si, Al, and Co central atoms and MFI type heterosilicates with Al, Ga, Fe, and B heteroatoms). For protons confined within small voids of heterosilicates, the transition state stabilization and reactivity depend additionally on van der Waals interactions that are unrelated to acid strength.

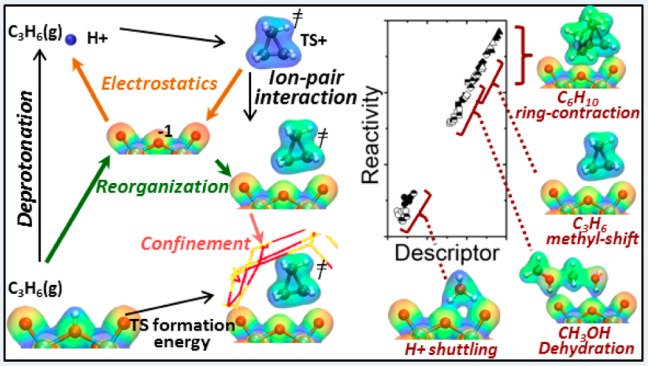

KEYWORDS: *thermochemical cycles, proton shuttling, dehydration, Brønsted acid catalysis, noncovalent interactions, isomerization, protonation*

Catalysis on solid Brønsted acids involves proton transfer to intermediates in order to form ion-pair transition states stabilized by interactions between a cation and the conjugate anion of the acid.[1,2] These proton transfer events make acid strength, rigorously described by the deprotonation energy (DPE) of the neutral acid,[3] an essential but incomplete descriptor of reactivity. The stability of transition states depends, however, also on the ability of cations and anions to interact at the transition state, via electrostatic forces that depend on where the charges reside in the two ions and how such charges are able to reorganize. To date, descriptors for broad classes of reactions and solid acids that rigorously account for these properties remain unavailable.

Rate constants derived from measured catalytic turnover rates reflect differences between Gibbs free energies of the kinetically relevant transition states and the relevant precursor states. Reactivity descriptors must, therefore, reflect in turn how these differences change with the composition of catalysts and reactants. 2-Methylpentene (2MP) isomerization turnover rates are given by the rate equation[4]

$$\frac{r_{isom}}{[H^+]} = \frac{k_{isom}K_{ads}P_{2MP}}{1 + K_{ads}P_{2MP}} \quad (1)$$

with first-order ($k_{isom}K_{ads}$) and zero-order (k_{isom}) rate constants in 2MP pressure. Here, $k_{isom}K_{ads}$ reflects the free energy of the isomerization transition state relative to those for a bound proton and a gaseous reactant molecule (ΔG^{TS}), while k_{isom} reflects the difference between ΔG^{TS} and the 2MP adsorption free energy (ΔG^{ads}) on bare protons. Similarly, CH_3OH dehydration turnover rates on solid acids are given by[5]

$$\frac{r_{CH_3OH,dehyd}}{[H^+]} = \frac{k_{1st}P_{CH_3OH}}{1 + \frac{k_{1st}}{k_{zero}}P_{CH_3OH}} \quad (2)$$

with first-order (k_{1st}) and zero-order (k_{zero}) rate constants in CH_3OH pressure. Theory and experiments show that k_{1st} and k_{zero} reflect differences between the ΔG^{TS} values for dehydration

Received: May 18, 2016
Revised: June 30, 2016
Published: July 20, 2016

DOI: 10.1021/acscatal.6b01402
ACS Catal. 2016, 6, 5386−5392

and the ΔG^{ads} values for monomers and dimers of CH_3OH, respectively.[5]

For the reactions and transition states considered in this work, the entropic contributions to free energies are similar on solid acids of different compositions, suggesting that the effects of compositions on reactivity are fully described by changes in ΔE^{TS} and ΔE^{ads} values (details in section S6 in the Supporting Information). As a result, only ΔE values are considered in the discussion that follows.

We have previously addressed some aspects of the incompleteness of DPE as a catalyst descriptor,[6] which becomes apparent when it is used to describe ΔE^{TS} and ΔE^{ads} values for methanol dehydration on different families of polyoxometalate (POM) clusters, each based on W and Mo addenda atoms. More complete descriptors require that we dissect DPE values into their ionic and covalent components, because ion-pair transition states recover significant fractions of the ionic component of DPE but a very small fraction of the covalent part.[6] Here, we provide a concise description of the concepts and the framework used to develop these descriptors and demonstrate their generality by applying them to describe much broader ranges of acid-catalyzed reactions and families of solid acids.

Thermochemical cycles, such as those shown in Scheme 1, dissect the energy required to form a transition state (TS) into components that depend on the properties of the solid acid and of the reactive species.[7] This activation energy, referenced in this case to a bound proton and a gaseous reactant (ΔE^{TS}, Scheme 1), depends on DPE, on the energy to form a gaseous TS analogue (TS^+) from gaseous H^+ and reactants (E_{prot}), and on the interaction energy of TS^+ with conjugate anions (E_{int}^{TS}):

$$\Delta E^{TS} = \mathrm{DPE} + E_{prot} + E_{int}^{TS} \quad (3)$$

These cycles rigorously describe the observed linear dependence of experimental and DFT-derived activation energies with the DFT-derived DPE values for solid acids, while providing a mechanistic interpretation for the attenuation of DPE effects on activation energies ($d\Delta E^{TS}/d\mathrm{DPE} < 1$) based on the fraction the DPE recovered by ion-pair interactions at transition states.[1,4,5] The TS^+ species were used as hypothetical constructs convenient in establishing reactivity–DPE relations. Their energies, however, can be derived explicitly by carrying out fully relaxed transition state calculations for gaseous cations undergoing the same structural rearrangement as the bound cation, but in the absence of a conjugate anion.[6] Such gas-phase calculations allow direct calculation of E_{prot} as the energy to form gaseous TS^+ from gaseous reactants, and of E_{int}^{TS} values from energy differences between gaseous and anion-bound transition states in the present study.

E_{prot} is a property of gaseous species and thus unaffected by properties of the solid acid. As a result, $\Delta E^{TS} - E_{prot}$ values depend on the properties of the solid only through its DPE and its ability to recover, in part, this energy through TS^+–anion interactions (i.e., DPE > 0; $E_{int}^{TS} < 0$),

$$\Delta E^{TS} - E_{prot} = \mathrm{DPE} + E_{int}^{TS} \quad (4)$$

DPE and E_{int}^{TS} reflect the ability of a given conjugate anion to stabilize H^+ and TS^+. When E_{int}^{TS} depends only on DPE, $\Delta E^{TS} - E_{prot}$ becomes a single-valued function of DPE, making DPE a full descriptor of reactivity.

Energies of adsorbed species at acid sites also depend on DPE and ion-pair interactions, as shown previously for species involved in CH_3OH dehydration.[6] When reference states consist of such adsorbed reactants (eqs 1 and 2)), their formation is rigorously considered by separate thermochemical cycles for ΔE^{ads}, in addition to that for ΔE^{TS} (in Scheme 1).[6] The concepts and the descriptors that we develop here for transition states can then be transferred without modifications to estimate activation energies referenced to adsorbed precursors.

Theory and experiment have previously demonstrated that measured rate constants and DFT-derived ΔE^{TS} values for dehydration and isomerization reactions depend only on DPE for each given type of solid acids.[1,5] A solid acid type is defined here as one containing protons balancing the charge of an oxoanion incorporated within a given solid oxide (e.g., S, P, Si, Al, and Co oxoanions in WO_x-based POM clusters; Figure 1). However, rate constants and ΔE^{TS} values for CH_3OH dehydration differ among different acid types exhibiting the same acid strength and DPE (e.g., POM with Mo and W addenda atoms but the same DPE; Figure 2a).[6] Such discrepancies arise because the energy required for cleaving covalent OH bonds via concomitant charge reorganization to form H^+ is greater on Mo than on W POM clusters, and the ion-pair TS structures recover a significant fraction of the H^+–O^- electrostatic attraction but only a small fraction of the reorganization energy.[6] Consequently, solid acids with less covalent OH bonds (e.g., W-POM) recover a larger fraction of the DPE upon formation of ion-pair TS structures, leading to lower ΔE^{TS} values for a given DPE in comparison to acids with more covalent OH bonds.

The ionic component of cation–anion interaction is accurately given by a classical electrostatic treatment of the energy involved in bringing an isolated cation and anion to their equilibrium distance, without allowing their charge distribution or the structure to relax into their minimum energy configuration. These ionic contributions can then be rigorously subtracted from DPE or E_{int}^{TS} values to obtain the additional energy involved in relaxing each ion in response to the presence of the counterion; this energy reflects covalent contributions to the energy of a proton or a transition state cation.[6] These ionic and covalent components represent quantitative descriptors of ion-pair

Scheme 1. Energy of a Methyl-Shift TS Referenced to a Bare Acid and a Gaseous C_3H_6 (ΔE^{TS}) Described in Terms of the Acid's DPE, the Gas-Phase Protonation Energy (E_{prot}), and Interaction Energy (ΔE_{int}^{TS}) of a Cationic TS Analogue with Conjugate Anion[a]

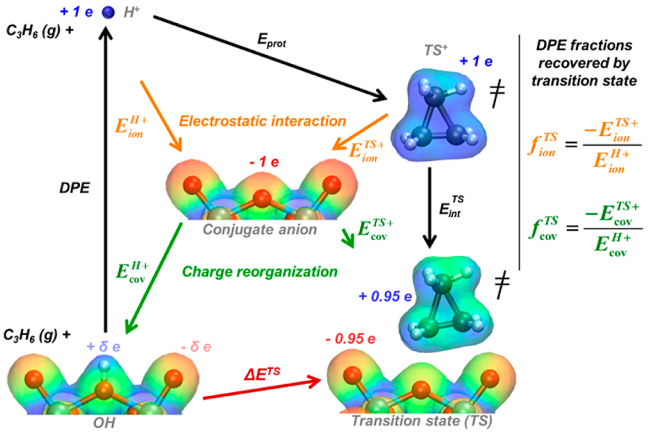

[a]DPE and ΔE_{int}^{TS} reflect ion-pair interactions with electrostatic (ionic) and charge reorganization (covalent) components. Colors for the electron distributions reflect electrostatic potentials.

DOI: 10.1021/acscatal.6b01402
ACS Catal. 2016, 6, 5386–5392

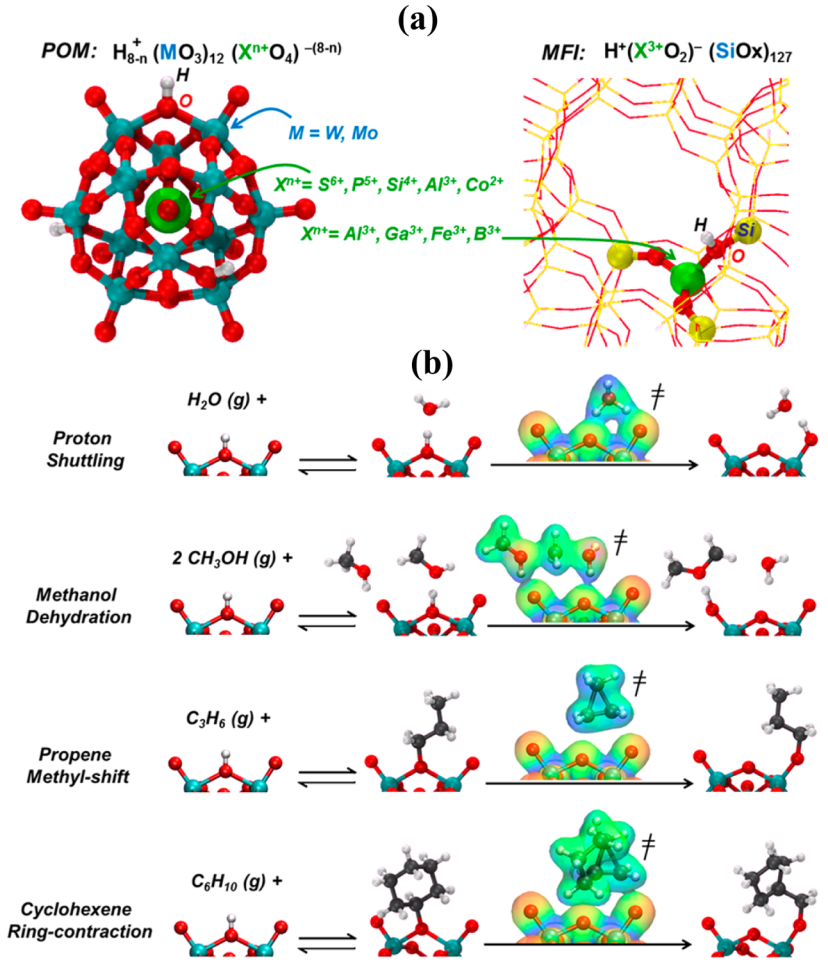

Figure 1. (a) Optimized structures of a $H_3PW_{12}O_{40}$ POM cluster and Al-MFI. The acid composition is modified by changing the heteroatom (X) in POM and MFI and all addenda atoms (M) in POM. (b) Optimized structures of TS, precursors, and products for H^+ shuttling, CH_3OH dehydration, C_3H_6 methyl shift, and C_6H_{10} ring contraction. Colors on electron distributions reflect electrostatic potentials.

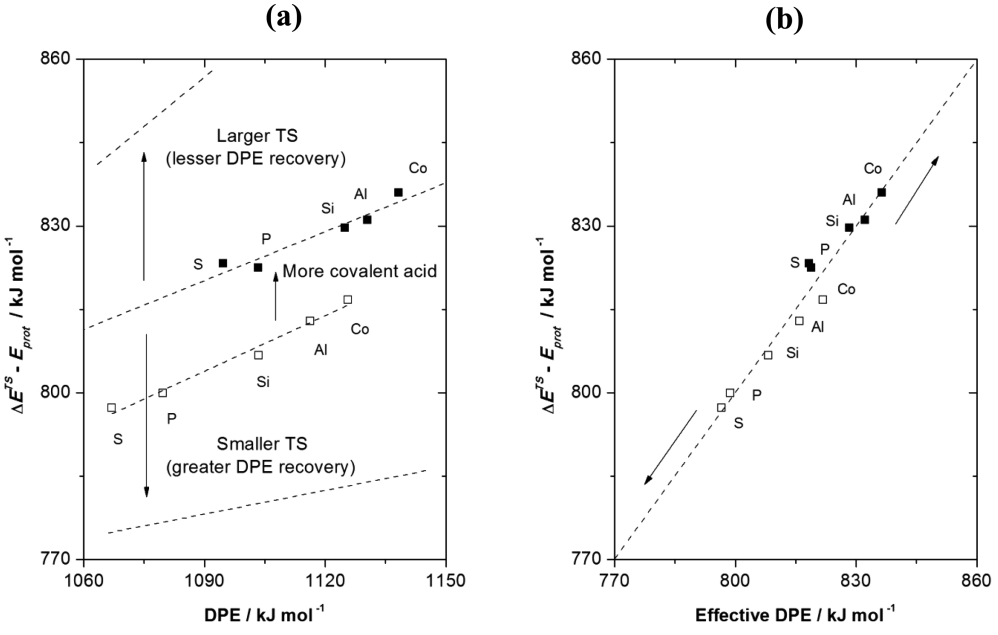

Figure 2. Difference between DFT-derived (PW91) TS energies and gas-phase protonation energies ($\Delta E^{TS}_{int} - \Delta E_{prot}$; Scheme 1) for CH_3OH dehydration on Mo (closed symbols) and W (open symbols) POM as a function of (a) DPE and (b) effective DPE. Dashed lines reflect best fits, expected trends (a), or the parity line (b).

DOI: 10.1021/acscatal.6b01402
ACS Catal. 2016, 6, 5386−5392

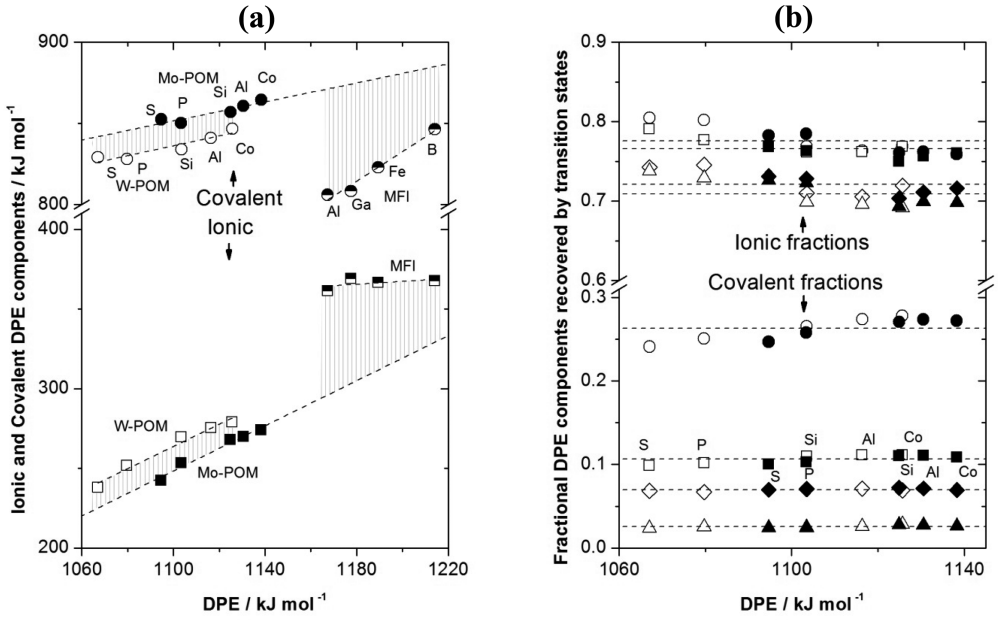

Figure 3. (a) Ionic (ΔE_{ion}^{H+}, squares) and covalent (ΔE_{cov}^{H+}, circles) components of the DPE of POM and MFI as a function of DPE values from DFT (PW91). Shaded regions reflect offsets between best-fit lines. (b) Fractions of ionic and covalent DPE components recovered by TS cations (f_{ion}^{TS},f_{cov}^{TS}) for H^+ shuttling (circles), CH_3OH dehydration (squares), C_3H_6 methyl shift (diamonds), and C_6H_{10} ring contraction (triangles) on W (open symbols) and Mo (closed symbols) POM as a function of DPE. Horizontal lines reflect averages over all POM clusters.

interactions, derived from formalisms describing partial covalency in ionic bonds as the ability of cations to polarize the excess charge in anions. The dependence of their magnitude on charge-to-size ratios of ions are consistent with Fajans' rules and with their fundamental underpinnings,[8−10] as previously described in detail.[6]

Alternate energy decomposition strategies seek to dissect the energy of a chemical bond into a "preparation energy", required to rearrange the structure and electron density of isolated fragments A and B to those in their bound A−B state, and an "interaction energy", recovered in bringing the "prepared" fragments together. These methods then decompose the interaction energy into "quasi-classical" electrostatic interactions between the fragments, Pauli repulsion between the wave functions of A and B, and an orbital mixing required to form the A−B wave function.[11−13] These methods describe chemical bonds in terms of components meaningful in the context of the equations required for ab initio descriptions of chemical bonds. They preclude the separation of ionic and covalent components of bond energies, as reflected in the significant quasi-classical electrostatic energies even for fully covalent bonds in homonuclear diatomic molecules;[13] they also give rise to extraneous energy components that are rendered unnecessary by the analysis protocols that we propose in the present study. Here, we determine the ionic component from the classical interactions between formal isolated ions, using electron distributions explicitly derived from DFT, and the covalent component, from the energy required to reorganize charge as a result of the mutual polarization by the interacting ions in a manner consistent with heuristic frameworks that link covalency with polarization.[10] These ionic and covalent components are then used here to develop more complete descriptors of reactivity in catalysis by solid acids.

A more general descriptor than DPE alone becomes evident when DPE and E_{int}^{TS} values in eq 4 for various acid types are separated into their ionic and covalent components (DPE = E_{ion}^{H+} + E_{cov}^{H+}; $E_{int}^{TS} = E_{ion}^{TS+} + E_{cov}^{TS+}$):

$$\Delta E^{TS} - E_{prot} = (E_{ion}^{H+} + E_{ion}^{TS+}) + (E_{cov}^{H+} + E_{cov}^{TS+}) \quad (5)$$

and the terms in parentheses are expressed as fractions of DPE components that are recovered upon the formation of a given TS (f_{ion}^{TS}, f_{cov}^{TS}; Scheme 1):[6]

$$\Delta E^{TS} - E_{prot} = E_{ion}^{H+}(1 - f_{ion}^{TS}) + E_{cov}^{H+}(1 - f_{cov}^{TS}) \quad (6)$$

Here, the f_{ion}^{TS} and the f_{cov}^{TS} values reflect ratios of respective ionic and covalent components of ion-pair interactions for protons (DPE) and transition states (E_{int}^{TS}):

$$f_{ion}^{TS} = \frac{-E_{ion}^{TS+}}{E_{ion}^{H+}} \quad (7)$$

$$f_{cov}^{TS} = \frac{-E_{cov}^{TS+}}{E_{cov}^{H+}} \quad (8)$$

These terms are then calculated explicitly for each combination of transition state and acid on the basis of DFT-derived energies and charge distributions of bound species and isolated ions. A f_{ion}^{TS} value smaller than unity represents a gaseous cation transition state that interacts less strongly than a proton with a given conjugate anion at their optimum electrostatic interaction distance without geometric or electronic perturbations. Similarly, a f_{cov}^{TS} value smaller than unity indicates that the energies associated with structural or electronic relaxations during the transformation from a gaseous to a bound transition state are smaller than for the corresponding relaxations in a proton. The $\Delta E^{TS} - E_{prot}$ values in eq 6 for CH_3OH dehydration on Mo and W POM become a single-valued function of $E_{ion}^{H+}(1 - f_{ion}^{TS}) + E_{cov}^{H+}(1 - f_{cov}^{TS})$ values that reflect an effective DPE described by the right-hand side of eq 6 (Figure 2b).[6] If f_{ion}^{TS} and f_{cov}^{TS} values did not depend on the DPE or the acid type and were unique for a given TS^+, the effective DPE would become a universal

DOI: 10.1021/acscatal.6b01402
ACS Catal. 2016, 6, 5386−5392

descriptor of reactivity that fully accounts for the relevant properties of the solid acid and of the reactive species involved.

We examine this hypothesis by calculating the values of f_{ion}^{TS} and f_{cov}^{TS} and confirming their invariance with DPE and with acid type. DFT-derived TS energies for H_2O-assisted H^+ shuttling, CH_3OH dehydration, C_3H_6 methyl shifts, and C_6H_{10} ring contraction are calculated from their respective gaseous reactants and bare protons at a single site on (Mo,W) POM and on heterosilicate clusters with the MFI framework and different framework heteroatoms (Al, Ga, Fe, B) (Figure 1). These systems represent diverse acid types covering the range of OH covalency of solid acids used in practice, as well as a practical range of size and recovery fractions of TS structures. Calculations were first performed using PW91[14] functionals that do not substantially account for van der Waals interactions (vdW) and then using vdW-DF2[15] functionals to probe the vdW stabilization of H^+ and TS^+ on POM and within MFI voids.

The DPE and its ionic and covalent components vary with the identity of the heteroatom or of the oxide incorporating them (Figure 3a). DPE values increase as the valence of the central atom decreases in W (1067 to 1126 kJ mol^{-1}) and Mo (1094 to 1128 kJ mol^{-1}) POM acids and as the identity of trivalent framework cation varies in MFI (1167 to 1214 kJ mol^{-1}). On all acids, the ionic component of DPE (E_{ion}^{H+}, 200−400 kJ mol^{-1}) is much smaller than the covalent component (E_{cov}^{H+}, 800−900 kJ mol^{-1}), as expected for the heterolytic cleavage of a largely covalent OH bond. Such bonds are most covalent in Mo POM and least covalent in MFI (Figure 3a), consistent with their DFT-derived HOMO−LUMO gaps (1.8, 2.5, and 5.6 eV for Mo and W POM and MFI, respectively; Supporting Information) and with the weaker charge reorganization possible for insulating solids.

TS cations recover significant fractions of the ionic component of DPE (f_{ion}^{TS} = 0.7−0.8; Figure 3b) but a much smaller fraction of its (larger) covalent component (f_{cov}^{TS} = 0−0.3; Figure 3b), consistent with the ubiquitous ion-pair character of the transition states that mediate acid catalysis. For these TS^+ species, both ionic and covalent recovery fractions increase as cations become smaller and approach the size of H^+ ($f^{\text{ring contraction}} < f^{\text{methyl shift}} < f^{CH_3OH\text{ dehydration}} < f^{H^+\text{ shuttling}}$). The recovery fractions for each TS^+ depend only weakly on DPE and are similar on Mo and W POM clusters, suggesting that they are unique properties of the cation and do not depend on acid identity or strength (Figure 3b). These fractions and formation energies of TS^+ species from a free H^+ (E_{prot}) are shown in Table 1.

Figure 4a shows DFT-derived $\Delta E^{TS} - E_{prot}$ values as a function of DPE (eq 4) for POM and MFI acids. For a given acid strength and type, these values are much smaller for H^+ shuttling than for C_6H_{10} ring contraction, because the larger f values of smaller TS^+ species lead to their more effective stabilization by conjugate anions. For a given DPE and TS^+, $\Delta E^{TS} - E_{prot}$ values are smaller on heterosilicate MFI structures (shaded regions, Figure 4a), which exhibit larger ionic components of DPE, than on W and Mo POM acids (Figure 3a), because TS^+ species recover a larger fraction of such ionic components than of the covalent ones (Figure 3b).

Table 1. Calculated Gas-Phase Protonation Energies (PW91) and Average Ionic and Covalent Recovery Fractions and Standard Deviations on POM Clusters for Transition States Shown in Figure 1

transition state	E_{prot} (kJ mol^{-1})	f_{ion}^{TS}	f_{cov}^{TS}
H^+ shuttling	−717	0.78(±0.017)	0.26(±0.013)
CH_3OH dehydration	−815	0.77(±0.011)	0.11(±0.005)
C_3H_6 methyl shift	−750	0.72(±0.015)	0.07(±0.002)
C_6H_{10} ring contraction	−815	0.71(±0.018)	0.03(±0.002)

This treatment shows that DPE values remain incomplete reactivity descriptors without their dissection into ionic and covalent components and a rigorous assessment of how TS cations (and any relevant adsorbed precursors) recover each part. These recovery fractions are essentially independent of the identity and DPE of the solid acid. As a result, they become a single-valued descriptor of the properties required to describe the stability of a given TS. These findings lead to a general descriptor in the form of an effective DPE value ($E_{ion}^{H+}(1 - f_{ion}^{TS}) + E_{cov}^{H+}(1 - f_{cov}^{TS})$, eq 6), which brings together the acid (E_{ion}^{H+}, E_{cov}^{H+}) and the TS (f_{ion}^{TS}, f_{cov}^{TS}) properties in their most general forms. $\Delta E^{TS} - E_{prot}$ values are shown in Figure 4b as a function of the values of this general descriptor obtained using E_{ion}^{H+} and E_{cov}^{H+} values for each acid (Figure 3a) and f_{ion}^{TS} and f_{cov}^{TS} values for each TS^+ (Table 1). The single-valued character shown by these data indicates that eq 6 accurately separates the properties of the anion (the solid) and the cation (the reaction chemistry and its TS) and then combines them to predict TS stability and thus reactivity. The general nature of these relations leads us to infer that the reactivities of all solid acids for which the E_{ion}^{H+} and E_{cov}^{H+} components of DPE are known or can be accurately predicted for any new reaction by calculating the f_{ion}^{TS} and f_{cov}^{TS} values of its TS on one such solid acid. Conversely, the reactivity of a new acid type can be accurately described by estimating its E_{ion}^{H+} and E_{cov}^{H+} components of DPE for any reaction for which f_{ion}^{TS} and f_{cov}^{TS} values are known. The procedures developed here for describing reaction-independent acid properties and acid-independent properties of reactions and for using them to assess trends in activation energies for other materials and reactions are summarized in section S7 of the Supporting Information.

We note that MFI acids, containing voids of molecular sizes, are also included in this "universal" relation, in spite of their ability to stabilize TS structures through vdW interactions.[16−18] Such surprising "universality" reflects the absence of vdW descriptors in the PW91 functionals used, a matter that is addressed next by using vdW-DF2 functionals that include the relevant dispersion forces.

PW91 and vdwDF2 give similar values for DPE and for ionic and covalent components on POM and MFI acids, as expected from the negligible effects of vdW interactions for protons (Figure 5a) and consistent with the ability of both functionals to describe similarly all energy components except those related to vdW forces. $\Delta E^{TS} - E_{prot}$ values for CH_3OH dehydration from PW91 and vdW-DF2 are similar for any given POM cluster (Figure 5b), suggesting that TS^+ experiences similar vdW stabilization in its gaseous and interacting forms, at least for conjugate anions with convex surfaces that do not provide strongly confining voids. In contrast, $\Delta E^{TS} - E_{prot}$ values derived from vdW-DF2 are ∼50 kJ mol^{-1} smaller for MFI structures than predicted by the trends in Figure 5b for all acids without vdW corrections. These offsets reflect the added stabilization of TS structures within voids of molecular dimensions, which are unrelated to acid strength. Such effects vary with DPE values and with confining locations within MFI and other heterosilicate frameworks; therefore, they must be calculated for each and must be done using functionals unavailable until recently.[19] Heterosilicates differ from POM in both their confining effects and their more ionic OH bonds.

DOI: 10.1021/acscatal.6b01402
ACS Catal. 2016, 6, 5386−5392

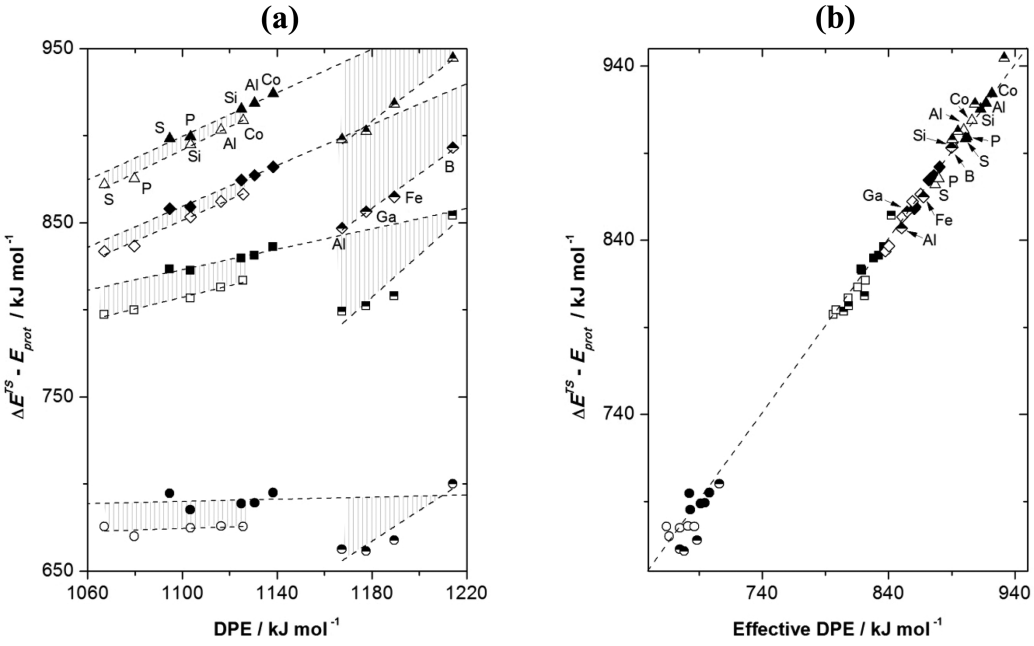

Figure 4. Difference between DFT-derived (PW91) TS energies and gas-phase protonation energies (ΔE_{int}^{TS} - ΔE_{prot}, Scheme 1) for H^+ shuttling (circles), CH_3OH dehydration (squares), C_3H_6 methyl shift (diamonds), and C_6H_{10} ring contraction (triangles) on Mo (closed symbols) and W (open symbols) POM and MFI (half-open symbols), as a function of (a) DPE and (b) effective DPE. Shaded regions reflect offsets between best-fit lines.

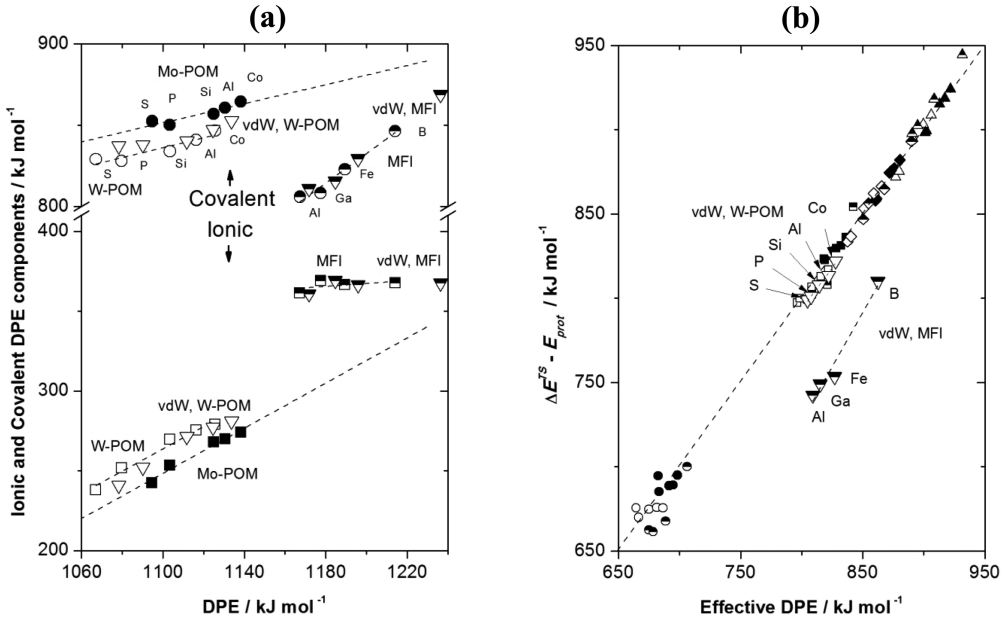

Figure 5. (a) Ionic and covalent DPE components as a function of DPE values derived from PW91 and vdW-DF2 functionals on POM clusters and MFI. (b) Effect of vdW functionals on $\Delta E^{TS} - \Delta E_{prot}$ values for CH_3OH dehydration as a function of effective DPE. All vdW values are shown by downward triangles; other symbols and conventions are identical with those in Figures 2a and 3b.

COMPUTATIONAL METHODS

DFT calculations were performed within the Vienna ab initio simulation package using PW91[14] and vdw-DF2[15] functionals, ultrasoft pseudopotentials,[20] 396 eV energy cutoffs, dipole/quadrupole corrections for all systems, and a uniform compensating charge and accompanying energy corrections for charged supercells. Energies and forces on atoms in relaxed structures were converged to within 10^{-6} eV and 0.05 eV A^{-1}, respectively. TS structures were obtained using the nudged elastic band[21] and dimer[22] methods. Electrostatic interactions were calculated by integrating over Coulomb energy terms for cation and anion distributions[6] (details in the Supporting Information).

ASSOCIATED CONTENT

Supporting Information

The Supporting Information is available free of charge on the ACS Publications website at DOI: 10.1021/acscatal.6b01402.

Details of DFT methods, structures of MFI clusters, procedures for calculation of electrostatic interaction energy between ions, ionic and covalent components of the DPE and the ion-pair interactions between transition

DOI: 10.1021/acscatal.6b01402
ACS Catal. 2016, 6, 5386−5392

states, DFT-derived HOMO−LUMO gaps in POM and MFI clusters, calculation of enthalpies and entropies using statistical mechanics treatments, and a summary of procedures for determining ion-pair interactions and using them for predictive guidance on reactivity trends (PDF)

AUTHOR INFORMATION

Corresponding Author

*E.I.: tel, +1-925-323-5559; fax, +1-510-642-4778; e-mail, iglesia@berkeley.edu.

Notes

The authors declare no competing financial interest.

ACKNOWLEDGMENTS

We thank William Knaeble (UC Berkeley) for helpful discussions, the U.S. Department of Energy (grant DE-AC05-76RL01830) for financial support, and the Environmental Molecular Sciences Laboratory of the Pacific Northwest National Laboratory (proposal 48772) and the XSEDE Science Gateways program (CTS150005) for computational resources.

REFERENCES

(1) Macht, J.; Janik, M. J.; Neurock, M.; Iglesia, E. *J. Am. Chem. Soc.* **2008**, *130*, 10369−10379.
(2) Yaluris, G.; Rekoske, J. E.; Aparicio, L. M.; Madon, R. J.; Dumesic, J. A. *J. Catal.* **1995**, *153*, 54−64.
(3) Brändle, M.; Sauer, J. *J. Am. Chem. Soc.* **1998**, *120*, 1556−1570.
(4) Knaeble, W.; Carr, R.; Iglesia, E. *J. Catal.* **2014**, *319*, 283−296.
(5) Carr, R. T.; Neurock, M.; Iglesia, E. *J. Catal.* **2011**, *278*, 78−93.
(6) Deshlahra, P.; Carr, R. T.; Iglesia, E. *J. Am. Chem. Soc.* **2014**, *136*, 15229−15247.
(7) Aronson, M. T.; Gorte, R. J.; Farneth, W. E. *J. Catal.* **1986**, *98*, 434−443.
(8) Fajans, K. *Naturwissenschaften* **1923**, *11*, 165−172.
(9) French, S. J. *J. Chem. Educ.* **1936**, *13*, 122−130.
(10) Geerlings, P.; De Proft, F. *Phys. Chem. Chem. Phys.* **2008**, *10*, 3028−3042.
(11) Ziegler, T.; Rauk, A. *Theoret. Chim. Acta (Berl.)* **1977**, *46*, 1−10.
(12) Krapp, A.; Bickelhaupt, F. M.; Frenking, G. *Chem. - Eur. J.* **2006**, *12*, 9196−9216.
(13) Frenking, G.; Krapp, A. *J. Comput. Chem.* **2007**, *28*, 15−24.
(14) Perdew, J. P. In *Electronic Structure of Solids '91*;. Ziesche, P., Eschrig, H., Eds.; Akademie Verlag: Berlin, 1991; pp 11−20.
(15) (a) Lee, K.; Murray, É. D.; Kong, L.; Lundqvist, B. I.; Langreth, D. C. *Phys. Rev. B: Condens. Matter Mater. Phys.* **2010**, *82*, 081101. (b) Klimes, J.; Bowler, D. R.; Michelides, A. *J. Phys.: Condens. Matter* **2010**, *22*, 022201.
(16) Sastre, G.; Corma, A. *J. Mol. Catal. A: Chem.* **2009**, *305*, 3−7.
(17) Corma, A. *J. Catal.* **2003**, *216*, 298−312.
(18) Eder, F.; Lercher, J. A. *J. Phys. Chem. B* **1997**, *101*, 1273−1278.
(19) Jones, A. J.; Zones, S. I.; Iglesia, E. *J. Phys. Chem. C* **2014**, *118*, 17787−17800.
(20) Vanderbilt, D. *Phys. Rev. B: Condens. Matter Mater. Phys.* **1990**, *41*, 7892−7895.
(21) Henkelman, G.; Jónsson, H. *J. Chem. Phys.* **2000**, *113*, 9978−9985.
(22) Henkelman, G.; Jónsson, H. *J. Chem. Phys.* **1999**, *111*, 7010−7022.

DOI: 10.1021/acscatal.6b01402
ACS Catal. 2016, 6, 5386−5392